Stability of Microstructure in Al3003 Builds made by Very High Power Ultrasonic Additive Manufacturing

K. Sojiphan, M.R. Sriraman, and S.S. Babu
Welding Engineering Program, Department of Materials Science and Engineering,
The Ohio State University, Columbus, OH 43221, USA

Abstract

Very High Power Ultrasonic Additive Manufacturing (VHP-UAM) system was used to produce aluminum parts from 150 μm thick Al3003-H18 foils. The build was processed at 36 μm vibration amplitude, 8 kN normal load, and 35.6 mm/s weld speed at 20 kHz frequency. Almost 100% linear weld density was achieved. A deformation-interaction volume of ~20 μm was observed below the bonded interface. The microstructural stability including grain boundary structures, and crystallographic orientations was evaluated after annealing these samples at $343^{o}C$ for 2 hours and $450^{o}C$ for 2 hours. After heat treatment, small grains persisted at the interfaces with sluggish grain growth kinetics. In contrast, normal grain growth kinetics was observed in the middle of the foils. Possible mechanisms for such phenomena are discussed.

Introduction

Ultrasonic additive manufacturing (UAM) or ultrasonic consolidation (UC) process is a solid-state joining process developed by Solidica Inc., for fabrication of complex geometry parts [1]. The process relies on ultrasonic seam welding of thin foils of 100-200 μm in thickness with high ultrasonic frequency of 20 kHz, and low amplitude of 14-28 μm. After a strip of foil is welded onto the base plate or substrate, another strip of foil is added and welded on top of the previous layer. The part can also be machined to create complex 3D features. This process has been used to fabricate industrial molds for injection molding, extrusion, and vacuum forming. Potential applications include encapsulating sensors and fibers as well as multi-material structures for advanced applications [1-10]. UAM is desired for additive manufacturing of the parts because no melting occurs during the process compared to other rapid prototyping processes [11].

The current UAM system is limited to bonding of soft face-centered-cubic (FCC) materials such as aluminum alloy. In order to weld higher strength materials (e.g. stainless steel, copper, titanium, nickel and iron alloys), Very High Power Ultrasonic Additive Manufacturing (VHP-UAM) system was developed by EWI. VHP-UAM has higher process capability of up to 15 kN normal force (7 times larger than UAM) and 52 μm vibration amplitude (twice higher than UAM). Recently, annealed 110-copper alloy build was fabricated by VHP-UAM process. The typical process parameters were 36 μm vibration amplitudes, 6.7 kN normal force, and 30 mm/s weld speed. After VHP-UAM processing, a grain reduction from up to 25 μm in as-received foil to ~0.3-10 μm was found near the interface. It is interesting to note that this grain size reduction occurred during processing without any post-process heat treatment. Therefore, Sriraman et al hypothesized the onset of dynamic recrystallization across the interface during processing [12].

Another goal of VHP-UAM is to minimize voids presented along the faying interfaces. In traditional UAM processing, this has been addressed by parameter optimization [5]. Recently, post-processing heat treatment was also shown to decrease the void fraction at the interface [13]. However, mechanical testing, of as-processed and heat-treated samples, has not been done to relate the reduction in void fraction to mechanical property improvement. Furthermore, a large grain size distribution was found across the UAM build after heat treatment [13]. In Al3003-H18 UAM build, large grains were found above the interfaces, while small grains remained below the interfaces after heat treatment at 343°C for 2 hours [13]. Such variations will affect mechanical properties of VHP-UAM parts. The goal of this research is to understand the stability of the microstructures evolved in a VHP-UAM processed build. The paper presents results from optical microscopy, microhardness testing, and electron backscatter diffraction (EBSD) analyses of both original Al3003-H18 foils and VHP-UAM build, before and after heat-treatment.

Experimental

Builds containing ten layers of 150 µm thick Al3003-H18 foils (Al-1Mn-0.7Fe-0.12Cu, by wt-%) on top of Al3003-H14 substrate were fabricated by VHP-UAM using different sets of processing parameters (vibration amplitude = 26 to 36 µm, normal load = 5.34 kN to 8 kN) at a welding speed=35.6 mm/s and vibration frequency of 20 kHz. Three samples were sectioned perpendicular to the weld/rolling direction (ND-TD plane) from the build processed at 36 µm amplitude and 8 kN load. One of the samples (referred to as VHP343) was heat treated at 343°C for 2 hours followed by air cooling. Another sample (referred to as VHP450) was heat treated at 450°C for 2 hours followed by air cooling. The third sample (referred to as VHP) was not heat-treated. The original Al3003-H18 foil (referred to as Foil) in the as-received condition as well as in the heat treated condition (343°C for 2 hours followed by air cooling) (referred to as F343) were also characterized across the ND-TD plane.

The foil, F343, VHP, VHP343, and VP450 samples were prepared using standard metallographic techniques. All the samples were sectioned carefully using thin diamond blade on a slow cutting machine across the ND-TD plane to avoid any introduction of plastic strains during sample preparation. They were then hot-pressed mounted using "Konductomet" bakelite and mechanically ground sequentially on 400, 600, 800, and 1200 grit SiC papers. The ground samples were polished using 3 µm diamond paste on the lecloth polishing cloth for ~30 minutes, and final-polished using 0.02 µm colloidal silica on the vibratory polisher for ~8-12 hours. After each grinding and polishing steps, samples were rinsed with water/distilled water, ultrasonically cleaned in ethanol/iso-propanol for ~2 minutes, and dried with warm/hot air dryer. It needs to be pointed out that sample preparation forms an important part to obtaining good results from the characterization techniques.

Optical images of as-processed VHP-UAM samples were obtained using Olympus-GX51 Optical Microscope. To quantify the bond quality, linear weld density (LWD) was measured [5, 13-14]. The LWD is the ratio of bonded area length to the total interface length [5]. In this work, a magnification of 1000X was used in conjunction with image analyses techniques to quantify LWD. Hardness measurements were done on each mounted sample using Leco AMH-43 microhardness machine. Vicker's indents with 25 g load were made along every interface and in

the middle of each foil layer of VHP-UAM samples to create hardness maps. At least twenty indents were made along each interface and middle of each layer.

EBSD analyses were performed on the XL-30 ESEM Field Emission Gun Scanning Electron Microscope at step sizes ranging from 0.2-1 μm. The SEM was set up at 15-20kV, spot size of 4-5, magnification of ~200X, and working distance ~22-26 mm. Data collection and data analyses were performed using TSL OIM software. The scans were made across layers near the top of each build. Small scan areas were made in the Al3003-H18 foil before and after heat treatment.

Results and Discussion

<u>Optical Microscopy</u>

Figure 1 shows the optical micrographs of VHP samples produced with different vibration amplitudes and normal loads. The images were taken across the ten layers and the substrate. In samples processed by traditional UAM (amplitude = 26 μm, normal force = 600-1000 N), the LWD is found to be in the range of 55-85% [14]. In VHP sample, while maintaining the amplitude at 26 μm (same as that of UAM) and increasing the normal force to 5340 N, the LWD increased to 98% (see Fig. 1-Left). Interestingly, by increasing vibration amplitude up to 36 μm (see Fig. 1-Right), LWD increased to ~99-100%. The results proved that VHP-UAM system has the capability to produce better bond in Al3003-H18 alloys.

The average thickness of each foil within the whole ten layer build was found to be ~135 μm (~ 10% reduction) after the VHP-UAM processing with higher amplitudes (36 μm). In contrast, only ~2% reduction in thickness was observed in samples processed with lower amplitude (26 μm). Such a reduction in thickness or plastic deformation could induce significant strain hardening in the build. In order to evaluate the extent of strain hardening, microhardness measurements were made on these builds.
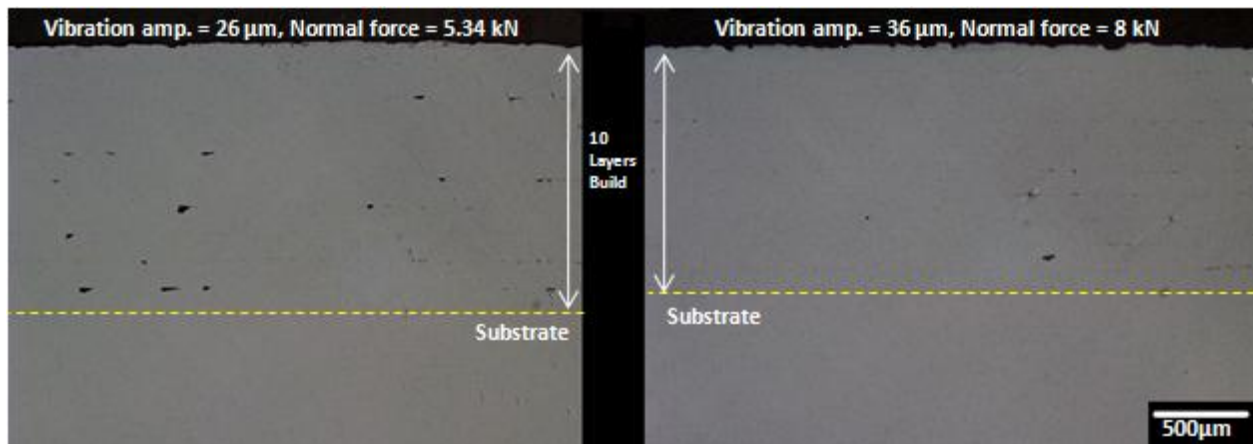

Figure 1: Optical Micrograph of VHP builds of Al3003-H18 processed with two different processing conditions resulting in different linear weld density. Left: Low VHP-UAM Parameter setting; LWD is equal to 98%; Right: Optimum VHP-UAM Parameter Setting; LWD is equal to 99-100%.

Hardness Measurement

Figure 2 shows the summary of Vicker's microhardness results of all samples before and after heat treatment. In contrary to our original hypothesis of strain hardening, the builds showed softening. The average hardness of the VHP sample was 57 VHN in comparison to 70 VHN of the Foil sample. The average hardness along the interfaces was found to be slightly higher than the average hardness in the middle of the foil. This is evident from the bimodal curve in the hardness data [see Fig. 2]. In contrast, in the samples processed at lower amplitude (e.g. sample in the left of Fig. 1), the average hardness of the VHP-UAM foils was found to be approximately the same as the original foil hardness. It is noteworthy that the average hardness of the samples produced by traditional UAM results is slightly higher than the original foil [13, 15]. This result suggests that the VHP-UAM processes are similar to a high temperature thermomechanical processing, however, constrained to the interface regions.

After heat treatment, the average hardness of both VHP-UAM builds and original foils decreased to ~40 VHN. No additional softening was found on increasing the heat treatment temperature from 343°C to 450°C. This indicated that the lowest possible hardness had been attained in the annealed samples.
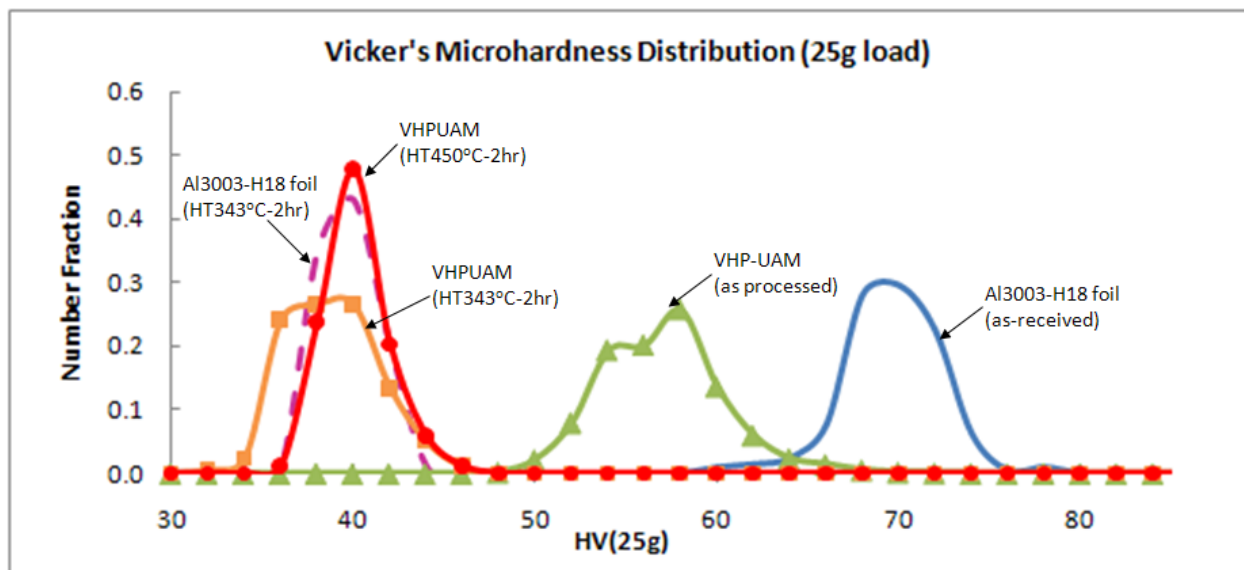

Figure 2: Microhardness distributions from Foil, F343, VHP, VHP343, and VHP450 samples

Electron Backscatter Diffraction (EBSD)

In order to understand the effect of post-processing heat treatment on the VHP-UAM builds, EBSD analyses of Foil, F343, VHP, VHP343, and VHP450 samples were performed. Figure 3 shows the inverse pole figure images of Foil and F343 sample. The as-received foil contained cold-rolled band or pancake structures with the average equivalent grain diameter less than 1 μm. In F343 samples, the pancake structures transformed into the equiaxed grains with the average diameters ~6 μm through recrystallization and grain growth mechanism.
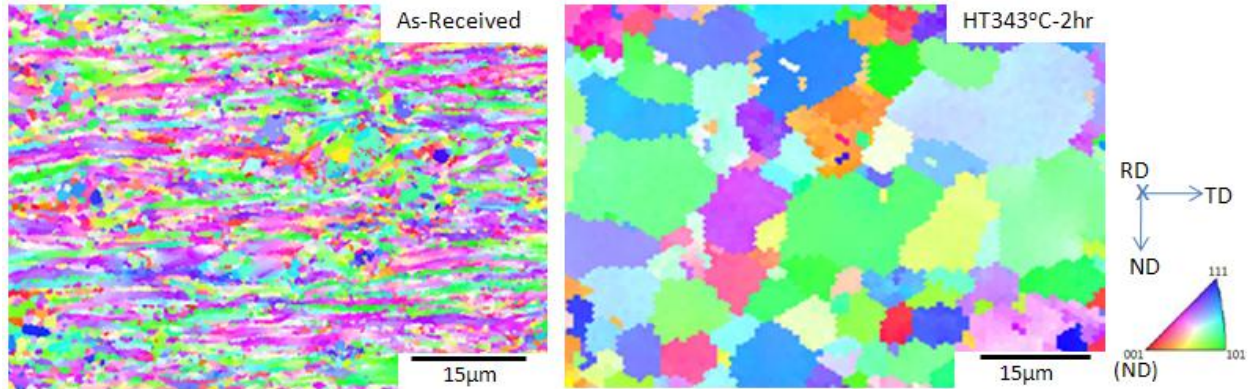
Figure 3: EBSD Inverse Pole Figure Images of Foil (0.2 μm step size) and F343 sample (1 μm step size).

Figure 4 shows the inverse pole figure images of VHP-UAM build in VHP, VHP343 and VHP450 samples. In the VHP sample, the scan was made across a few layers below the top surface of the build. For VHP343 and VHP450 samples, the scans were made from the first layer from the top to the third layer below.

In the VHP sample, three different regions were identified based on the inverse pole figure image (see Fig. 4-Left). In Region I, extremely fine equiaxed grains with diameter less than 1 μm were observed. This region is at 20 μm below the interface. Based on the published results, this is attributed to dynamic recrystallization phenomena [12-13, 16]. In Region II, a significantly large deformation-interaction zone was observed. The size of Region II was ~50 μm below Region I. This is delineated by a sudden change in the crystal orientations. Crystal or grain rotations were evident where layers of grains in the near-111-orientation (navy blue) on the ND-TD plane emerged after VHP-UAM processing. This orientation was not as evident in the Foil sample. Interestingly, recent EBSD results from VHP-UAM builds processed at lower amplitude and normal force showed no interaction zone with near-111-orientation band [17]. Based on the above observations, Region II is believed to be the area where large plastic deformation occurred due to an increase in normal load. Lack of fine recrystallized grains suggests that the deformation here was not accompanied with any adiabatic heating as opposed to Region I. In Region III, relatively low plastic deformation was expected as compared to Region II. Nevertheless, slight crystal orientation changes were observed. The size of Region III extended ~60 μm below Region II. Currently the above results are being evaluated further with detailed and quantitative texture analyses [17].

The results are more interesting in the VHP343 sample. The sample contains alternating large and small grains with varying crystal misorientations, as function of build height (see Fig. 4-Middle). In the top-most layer, a substantially large region shows a grain size greater than 100 μm above the foil-foil interface. Above this region, small grains seemed to dominate. In contrast, in the second layer from the top surface, small grains dominated in the region up to 80 μm below the top foil-foil interface, while large grains dominated in the region of 50 μm above the bottom foli-foil interface. Based on depth information, the large grain region in the second layer came from Region III in VHP sample. In the third layer from the top foil-foil interface, small grains dominated at least 70 μm below the interface, similar to the second layer from the top. The EBSD scans were not repeated below the top three layers. However, based on optical

microscopy of etched samples [17], we speculate that similar patterns will be repeated in the layers below. Intriguingly, the large grains in VHP343 sample had an average diameter > 20 μm, which is much larger than the grain size in the F343 sample.

In VHP450 sample, almost the whole volume consists of very large grains (see Fig. 4-Right). Most of these grains had grain diameters larger than 50 μm. Interestingly, small grains still persists close to foil-foil interface. However, the fractions of these fine-grains are much lower than that of VHP343 samples. This suggests that these small grains at the interface are being consumed by sluggish grain growth phenomena. In contrast, rapid grain growth kinetics is observed in the bulk regions of the VHP-UAM foils. Presence of persistent small grains near the interface was also observed in samples processed by traditional UAM after similar heat-treatment [13].
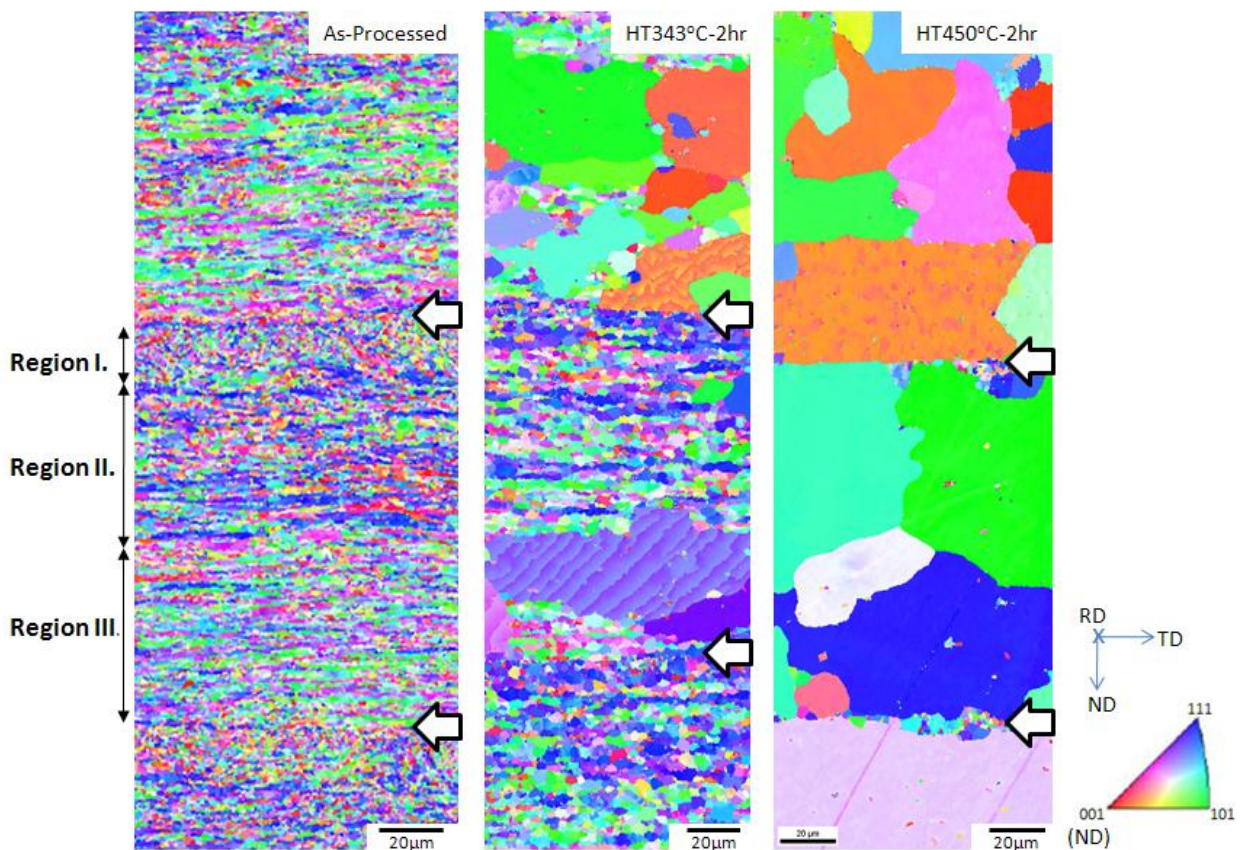

Figure 4: EBSD Inverse Pole Figure Images of (Left) VHP sample– a few layers below top surface in the as-processed Al3003H18 VHP-UAM build (0.3 μm step size), (Middle) – the top three layers of VHP343 sample (0.3 μm step size), and (Right) – the top three layers of VHP450 sample (0.35 μm step size). The arrows indicate the possible locations of original foil-foil interfaces

Discussion on VHP-UAM Processing-Microstructure-Property Correlations

In order to understand the stability of microstructures in UAM builds, we need to consider time history of thermal-mechanical cycles during UAM processes. Previous researches proposed several possible mechanisms that could occur during such thermal-mechanical cycles [12-13, 16, 18]. One of the most important mechanisms is the on-set of dynamic recrystallization in the vicinity of the interfaces. These are the regions expected to undergo a high-strain rate

plastic deformation due to asperity collapse [12-13, 16]. Adiabatic heating due to high-strain rate plastic deformation may aid the dynamic recrystallization process [12, 16]. In the bulk of the foils, large amount of low angle boundaries were observed in the UAM build. These phenomena were proposed as dynamic recovery by sub-grain rotations [18].

In the VHP-UAM samples [see Fig. 4 (Left)], the size of dynamically recrystallized region extends 20 μm below the foil-foil interfaces (Region I). It is possible to relate these fine grained materials to that of the tribomaterial formed during sliding [19]. The roughness of the sonotrode surface is mentioned as R_A ~7 μm [12]. The actual topology of the surface however is not known. Consequentially, the depth of the interaction zone between the sonotrode and the foil could even be larger. Therefore, Region I cannot be attributed directly to surface-wear damage, but rather the combination of surface-wear damage and some material volume below. Temperature measurements along the foil-foil interfaces indicate a localized (60-120°C) temperature increase [20]. These values are within the range of $0.36T_m$ to $0.42T_m$. This localized temperature increase may trigger recrystallization at these interfaces. However, the exact sequence of this process in not yet clear. The dynamic recrystallization region could have occurred either during the sonotrode and top foil surface interaction (surface-wear damage) or during the joining between foils. Detailed step-by-step procedure should be performed to confirm microstructure evolution and is the subject of ongoing work.

The EBSD results show that the interface regions have fine grains. As per the Hall-Petch law these regions should show a substantial higher hardness from the foil. In contrary, we observe softening (see Fig. 2) in both interface and in bulk of the builds, in comparison to foil hardness. This softening was also reported in VHP-UAM of 110-copper alloy in hard-temper condition [12]. This is attributed to drastic changes in dislocation content of the builds due to recovery and recrystallization in the work-hardened (H18) aluminum foils during processing.

The driving force for recovery and recrystallization is related to stored energy [21]. It is known that 90% of energy expended during plastic deformation of metal by cold-working converts into heat, while only 10% is stored in the lattice and referred to as stored energy [22]. During VHP-UAM, thermo-mechanical deformation (TMD) conditions are expected under two conditions. First, TMD might have occurred during the foil-sonotrode interaction [16]. Secondly, the microstructure from this step will be modified by joining step during foil-foil interaction. As a result, the stored energy would increase at and below the interfaces, especially in Region I and Region II from both steps. However, because the stored energy is the driving force for both dynamic recovery and dynamic recrystallization during processing, the stored energy would be released and decreased as well. Unfortunately, whether the actual values of stored energy is increased or decreased during VHP-UAM process under in-situ conditions cannot be measured.

We believe that the spatial variation of stored energy can only be measured by understanding the stability of these regions under post-process heat treatment conditions. In support of this hypothesis, the EBSD data shows large variations of grain growth and evolution of misorientations. However, to quantify the stored energy after VHP-UAM processing, we need to rationalize the microstructure evolution through meso-scale grain growth simulation models [23]. These meso-scale simulation models can be run under different assumed stored energy

distribution in the builds. The simulations can be run iteratively until it matches the experimental microstructural distribution before and after isothermal heat-treatment conditions. This is the focus of the ongoing research.

Summary and Conclusions

The present work focused on the effect of VHP-UAM process and after-process heat treatment on the microstructure evolution within the VHP-UAM build. The results were compared to the original foil microstructure before and after similar heat treatment. The major findings are summarized as follows:

- At very high vibration amplitude and normal force in VHP-UAM, a LWD of close to 100% can be achieved with minimal voids present along the interfaces.
- At the current processing condition (36 μm amplitude, 8 kN load), softening of microstructure was found as the hardness of VHP-UAM build was much lower than the original foil hardness. The interface hardness was found to be slightly higher than the bulk of VHP-UAM layer hardness due to smaller grain sizes existed near the interfaces.
- Dynamic recrystallization was proposed as mechanism for extremely fine grains in the vicinity of the VHP-UAM interface while dynamic recovery by sub-grain rotation is possible mechanism in the bulk of VHP-UAM layers.
- After heat treatment at 343°C for 2 hours, small grains existed below the interfaces with large grains observed in the bulk. In the top-most layer, however, more number of large grains occurred. When heat treated at higher temperature (450°C), large grain growth occurred across almost the whole VHP-UAM foil width with much smaller regions of small grains existed at the interfaces. Although an increase in grain growth is expected with increased temperature, as was observed in the bulk, it is still not clear as to why the grains resist growth at the interface regions.
- The average grain diameter of heat-treated as-received foil was much smaller than the grains observed within the heat-treated VHP-UAM sample. This is indicative of the significant changes in stored energy, textures and grain boundary energies following VHP-UAM.

References

1. D.R. White. *Ultrasonic consolidation of aluminum tooling.* Advanced Materials & Processes. January 2003. Page 64-65.
2. C.Y. Kong, R.C. Soar, and P.M. Dickens. *Ultrasonic consolidation for embedding SMA fibers within aluminum matrices.* Composite Structures. Vol. 66. 2004. Page. 421-427.
3. C.Y. Kong, and R. Soar. *Method for embedding optical fibers in an aluminum matrix by ultrasonic consolidation.* Applied Optics. Vol. 44. No. 30. 2005. Page 6325-6333.
4. J. George, and B. Stucker. *Fabrication of lightweight structural panels through ultrasonic consolidation.* Virtual and Physical Prototyping. Vol. 1. No. 4. 2006. Page. 227-241.
5. G.D. Janaki Ram, Y. Yang, and B.E. Stucker. *Effect of process parameters on bond formation during ultrasonic consolidation of aluminum alloy 3003.* Journal of Manufacturing Systems. Vol. 25. No. 3. 2006. Page. 221-237.

6. G.D. Janaki Ram, C. Robinson, Y. Yang, and B.E. Stucker. *Use of ultrasonic consolidation for fabrication of multi-material structures.* Rapid Prototyping Journal. Vol. 13. No. 4. 2007. Page. 226-235.

7. R.B. Tuttle. *Feasibility study of 316L stainless steel for ultrasonic consolidation process.* Journal of Manufacturing Processes. Vol. 9. No. 2. 2007. Page. 87-93.

8. Y. Yang, G.D. Janaki Ram, B.E. Stucker. *An experimental determination of optimum processing parameters for Al/SiC metal matrix composites made using ultrasonic consolidation.* Journal of Engineering Materials and Technology. Vol. 129. 2007. Page. 538-549.

9. D. Li, and R. Soar. *Optimum process parameters and influencing factors for embedding SiC fibres in Al 6061 O matrix through ultrasonic consolidation.* Materials Science and Technology. 2007. Page. 3048-3064.

10. R. Hahnlen, M.J. Dapino, K. Graff, and M. Short. *Aluminum-matrix composites with embedded Ni-Ti wires by ultrasonic consolidation.* SPIE Smart Structures and Materials & Nondestructive Evaluation and Health Monitoring. 16th Annual International Symposium, San Diego, California, March 8-12, 2009.

11. N. Johnson. *Rapid Prototyping using Ultrasonic Metal Welding.* M.S. Thesis. Tufts University. 1998.

12. M.R. Sriraman, S.S. Babu, and M. Short. *Bonding Characteristics during Very High Power Ultrasonic Additive Manufacturing of Copper.* Scripta Materialia. Vol. 62. 2010. Page. 560-563.

13. D. Schick. *Characterization of Aluminum 3003 Ultrasonic Additive Manufacturing.* M.S. Thesis. The Ohio State University. 2009.

14. C.D. Hopkins. *Development and Characterization of Optimum Process Parameters for Metallic Composites made by Ultrasonic Consolidation.* M.S. Thesis. The Ohio State University. 2010.

15. D.E. Schick, et al. *Microstructural Characterization of Bonding Interfaces in Aluminum 3003 Blocks Fabricated by Ultrasonic Additive Manufacturing.* Welding Journal. Vol. 89. No. 5. 2010. Page. 105s-115s.

16. R. R. Dehoff and S. S. Babu. *Characterization of Interfacial Microstructures in 3003 Aluminum Alloy Blocks Fabricated by Ultrasonic Additive Manufacturing.* Acta Materialia, Vol. 58, pp. 4305-4315.

17. K. Sojiphan, S. S. Babu , unpublished research, The Ohio State University, Columbus, Ohio, 43221, 2010.

18. E. Mariani, and E. Ghassemieh. *Microstructure evolution of 6061 O Al alloy during ultrasonic consolidation: An insight from electron backscatter diffraction.* Acta Materialia. Vol. 58. Issue. 7. 2010. Page. 2492-2503.

19. D.A. Rigney, and S. Karthikeyan. *The Evolution of Tribomaterial During Sliding: A Brief Introduction.* Tribology Letters. Vol. 39. No. 1. 2010. Page. 3-7.

20. M. R. Sriraman, M. Gonser, H. Fujii, S. S. Babu, and M. Bloss, unpublished research, The Ohio State University, Columbus, Ohio, 43221, 2010.

21. F.J. Humphreys, and M. Hatherly, *Recrystallization and Related Annealing Phenomena,* Phenomena, Pergamon, Oxford, 1995.

22. G.E. Dieter. *Mechanical Metallurgy.* McGraw-Hill. New York, 1986.

23. G. B. Sarma, B. Radhakrishnan and P. R. Dawson, *Mesoscale Modeling of Microstructure and Texture Evolution During Deformation Processing of Metals*. Advanced Engineering Materials, 2002, Vol. 4. pp. 509 – 514.